The Extended Cross-Float Calibration Method

Adam Brzozowski [1,2], Piotr Gazda [1], Michał Nowicki [1]
[1] Warsaw University of Technology, Institute of Metrology and Biomedical Engineering, Faculty of Mechatronics, sw. A. Boboli 8, 02-525 Warsaw, Poland
[2] Central Office of Measures, Elektoralna 2, 00-139 Warsaw, Poland

Abstract: The Extended Cross-Float method introduced in this paper offers a faster and simpler route to calibrating pressure balances than the classical cross-float technique. Where the conventional method requires locating a hydrostatic equilibrium point through laborious, iterative mass adjustment, the proposed method removes that bottleneck entirely: it determines the effective area of the piston-cylinder assembly directly from the change in piston fall velocity, measured by laser sensors before and after a shut-off valve is opened. The measurement setup is the same standard and device-under-test arrangement already familiar to calibration laboratories, so the method is inexpensive to adopt and easy to integrate into existing workflows. Experimental validation on two purpose-built assemblies over a 10 bar to 60 bar range confirmed the working principle and demonstrated strong practical potential, both as a fast preselection tool that markedly shortens the search for the equilibrium point and as an independent check of calibration readiness. The approach is simple, low-cost, and quickly executed, and it opens a promising new route toward faster and more accessible pressure-balance calibration.

Keywords: piston balance calibration, deadweight tester calibration, pressure metrology, piston-cylinder calibration, extended cross-float

1. Introduction

Pressure Balance instruments are widely used measuring devices with a well-established standing, as they provide excellent metrological performance combined with highly stable characteristics. Their operating principle, based almost entirely on pure mechanical phenomena, makes them essential equipment in measurement and calibration laboratories, as well as in all applications where highly repeatable measurement results, high reliability, and minimal long-term drift are required [1, 2]. Furthermore, advances in precision manufacturing technologies have significantly improved the availability of measurement assemblies for pressure balances. Users now have increasingly easier access to a broad range of highly accurate measuring instruments. Consequently, the demand for the calibration of such pressure balances continues to grow [3]. The purpose of the present study is to propose a promising new calibration method that offers an attractive and practical alternative to the solutions currently in use [4, 5]. This approach is intended to provide calibration laboratories with a broader range of methodological options, enabling the selection of calibration procedures best suited to their specific requirements. A particularly appealing feature is that it removes the laborious equilibrium search of the classical cross-float method and replaces it with a fast, direct velocity measurement, which promises shorter calibration times and a lower entry threshold. The implementation-oriented nature of the developed method is intended to enhance the capabilities of calibration laboratories, both by introducing a novel approach to currently applied measurement methods and by serving as an additional internal tool for the verification and confirmation of calibration results obtained.

The novelty of this work can be summarized as follows: to the best of the authors' knowledge, this is the first calibration method for pressure balances in which the effective area is determined in a dynamic regime, so that the search for the hydrostatic equilibrium point – the defining and most laborious stage of the classical cross-float method – is eliminated entirely; a complete measurement model of such a dynamic comparison is formulated, including the medium, pressure-distortion, thermal and second-order correction factors, together with the corresponding uncertainty budget; the required instrumentation is limited to two low-cost laser displacement sensors added to the standard cross-float arrangement, which makes the method directly implementable in existing calibration laboratories.

Autor korespondujący:
Adam Brzozowski, adam.brzozowski@gum.gov.pl

Artykuł recenzowany
nadesłany 01.07.2026 r., przyjęty do druku 13.08.2026 r.

2. State of the art

The key parameter describing the assembly of a Pressure Balance is the effective area [6]. Determining its value constitutes the fundamental step in the calibration process of this type of instrument. Due to the design of the assembly, the effective area represents a resultant quantity dependent on both the piston diameter and the cylinder diameter. However, its determination is not a straightforward calculation because of the physical phenomena occurring within the clearance between the piston and the cylinder [7]. Although such determination is possible, it requires advanced mathematical methods as well as highly accurate geometric measurements [8]. Furthermore, the contribution of the uncertainty components associated with these measurements results in acceptable levels of combined uncertainty being achievable primarily for assemblies with relatively large diameters and comparatively low pressure ranges. As a consequence, the determination of the effective area of an assembly based on geometric measurements is, in practice, employed almost exclusively by national metrology institutes and mainly for standards of the highest accuracy classes [9, 10].

Probably the most widely used method for determining the effective area is the so-called cross-float method [11, 12]. It is based on an indirect comparison between a reference instrument and the calibrated instrument [13]. These two instruments are connected through a sealed pressure system. The key objective is to identify a hydrostatic equilibrium point at which each instrument operates in a manner close to its independent operation, when the piston fall rate in the interconnected system is identical to the piston fall rate of the instrument operating independently (isolated from the pressure system). This is the most difficult and most time-consuming stage of the calibration procedure. It requires the metrologist to have substantial experience in operating Pressure Balance instruments, highly stable environmental conditions, and precisely determined influence quantities affecting the measurement result, such as the masses of the weights used in the calibration, the local value of gravitational acceleration at the measurement site, the physico-chemical properties of the pressure-transmitting medium, and the height difference between reference levels [14]. Time consumption is also an important factor. Identifying the equilibrium point involves laborious mass adjustment through experimental iterations reaching a resolution of single milligrams.

All of this results in pressure balance calibration having a very high entry threshold, which for many calibration laboratories constitutes an insurmountable barrier. In turn, in laboratories that have decided to implement this type of service, it represents a factor significantly affecting the cost and, consequently, the final accessibility of the service.

3. Methodology

3.1. Calibration method description – measurement equation

As already mentioned, the key element in the classical cross-float method is the identification of the equilibrium point. When this condition is satisfied, the following relation holds true:

$$p_{\mathrm{ST}} = p_{\mathrm{DUT}} \tag{1}$$

The attainment of the equilibrium point is performed experimentally through gradual adjustment of the masses and observation of the effect of the applied change on the fall rate of the assemblies. The measurement system used in the cross-float method can be described as a hydraulic balance, which, in the absence of equilibrium, implies that when one piston descends, the other rises. The rate of these movements is correlated with the ratio between the applied masses and the effective areas of the pistons. The greater the imbalance, the higher the velocity of the resulting positional changes.

The starting point for implementing the Extended Cross-Float method is a measurement system identical to that used in the classical cross-float method. Two assemblies of Pressure Balance instruments, the standard (ST) and the device under

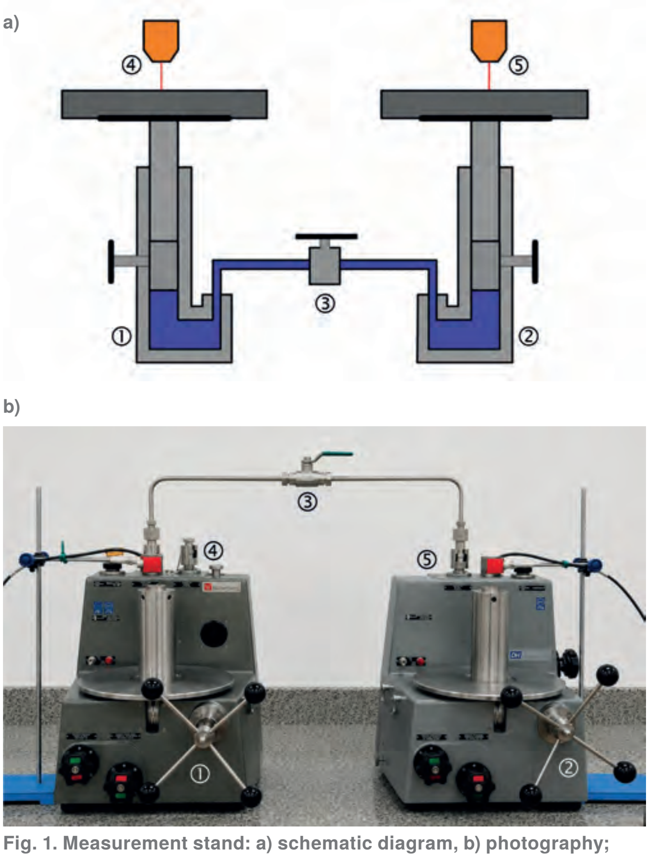

Fig. 1. Measurement stand: a) schematic diagram, b) photography; 1 – Standard, 2 – Device Under Test, 3 – cut-off valve, 4, 5 – laser sensors

Rys. 1. Stanowisko pomiarowe: a) schemat ideowy, b) fotografia; 1 – wzorzec, 2 – przyrząd wzorcowany, 3 – zawór odcinający, 4, 5 – czujniki laserowe

test (DUT), are connected within a single pressure system but separated by a shut-off valve.

In the beginning, the assemblies are brought to their operating position: the pistons are loaded with weights corresponding to the same nominal pressure, raised to the reference level, and set into rotation. The measurement setup is equipped with displacement sensors that continuously monitor the piston positions. With the shut-off valve closed, the operating pistons slowly descend due to the clearance between the piston and the cylinder, and the natural fall rate of both assemblies is recorded. Each piston is in a quasi-static force equilibrium, while beneath each piston the pressure is defined by the following equation:

$$p_i = \frac{M_i g_{\mathrm{loc}}\left(1-\frac{\rho_{\mathrm{air}}}{\rho_{M,i}}\right)}{A_{\mathrm{ef},i}} + \rho_{\mathrm{med}}\cdot g_{\mathrm{loc}}(h_{\mathrm{ref}}-h_i) + \frac{\sigma C_i}{A_{\mathrm{ef},i}} \tag{2}$$

where: $A_{\mathrm{ef},i}$ – piston effective area [m^2], M_i – mass of weights [kg], g_{loc} – local gravity [m/s^2], ρ_{air} – air density [kg/m^3], $\rho_{M,i}$ – weights density [kg/m^3], ρ_{med} – medium density (oil or gas) [kg/m^3], h_{ref} – reference level [m], h_i – reference level of the Piston-Cylinder Unit (PCU) [m], σ – medium surface tension (≡ 0 for gas) [N/m], C_i – piston circumference [m].

The operating piston gradually descends due to the loss of the pressure-transmitting medium in the measurement system, which results from the clearance within the assembly. The piston falls at a rate that follows the loss of the medium. Let v_0 denote the signed vertical piston velocity, taken positive upward, so that during the natural fall v_0 is negative; therefore:

$$A_{\text{ef}} \cdot v_0 = -Q_{\text{L}} \tag{3}$$

where: v_0 – natural flow rate [m/s], Q_{L} – annular clearance flow [m³/s].

The leakage flow rate Q_{L} depends on several parameters: the geometry of the clearance between the piston and the cylinder (length, width), the viscosity of the medium (and thus also temperature), the pressure beneath the piston (which drives the flow), and the rotational speed of the piston [15].

Next step of the measurement method is opening the cut-off valve. This results in the connection of the two previously separate pressure systems into a single united system. Each piston continues to generate pressure according to the equation given above. However, due to differences in pressure values, a medium flow is induced (there is a low probability of achieving equilibrium between the assemblies; in such a case, a deliberate imbalance must be introduced by adding a small mass on one side). Displacement sensors begin to record changes: one piston starts to rise (a reversal of motion direction), while the other begins to descend at a higher rate. This process continues until the pistons reach their mechanical end-stops, which prevent any further displacement.

For a liquid (assumed incompressible in the first approximation), the volumetric flow balance in the chamber beneath the piston after opening the valve is given by:

$$A_{\text{ef},i} \cdot v_i = -Q_{\text{L}} + \varepsilon_i \cdot Q_{\text{Z}} \tag{4}$$

where: v_i – piston flow rate after opening the valve [m/s], Q_{Z} – valve flow [m³/s], ε_i – sign based on the flow direction1: $\varepsilon_{\text{ST}} = -1$, $\varepsilon_{\text{DUT}} = +1$, (if $p_{\text{ST}} > p_{\text{DUT}}$).

In the case of a gaseous medium, the situation is different, as incompressibility cannot be assumed, and the compressibility of the gas is several orders of magnitude greater than that of oil.

By subtracting the equation for the closed valve from the equation for the open valve (for the same PCU):

$$A_{\text{ef},i} \cdot (v_i - v_{i,0}) = \varepsilon_i \cdot Q_{\text{Z}} \tag{5}$$

Defining the flow rate increment as $\Delta v_i = |v_i - v_{i,0}|$ (with the sign convention chosen such that Δv is always positive) – $\Delta v_{\text{ST}} = v_{\text{ST},0} - v_{\text{ST}}$ and $\Delta v_{\text{DUT}} = v_{\text{DUT}} - v_{\text{DUT},0}$ – the following is obtained:

$$A_{\text{ef,ST}} \cdot \Delta v_{\text{ST}} = Q_{\text{Z}} \tag{6}$$

$$A_{\text{ef,DUT}} \cdot \Delta v_{\text{DUT}} = Q_{\text{Z}} \tag{7}$$

Since Q_{Z} is the same flow rate (the same liquid passing through the same valve), we obtain the fundamental equation of the method:

$$A_{\text{ef,ST}} \cdot \Delta v_{\text{ST}} = A_{\text{ef,DUT}} \cdot \Delta v_{\text{DUT}} \tag{8}$$

Hence, the fundamental measurement equation is obtained:

$$A_{\text{ef,DUT}} = A_{\text{ef,ST}} \cdot \frac{\Delta v_{\text{ST}}}{\Delta v_{\text{DUT}}} \tag{9}$$

where: Δv_{ST} – standard flow rate increase: $\Delta v_{\text{ST}} = v_{\text{ST},0} - v_{\text{ST}}$ [m/s] (positive), Δv_{DUT} – DUT flow rate increase: $\Delta v_{\text{DUT}} = v_{\text{DUT}} - v_{\text{DUT},0}$ [m/s] (positive).

Since $A_{\text{ef,ST}}$ is known (based on the calibration certificate) and by measuring Δv_{ST} and Δv_{DUT} (using laser sensors), it is possible to calculate $A_{\text{ef,DUT}}$.

It should also be noted that the effective area depends on the pressure and temperature prevailing during the measurement. This dependence is modeled linearly:

$$A_{\text{ef},i}(p,T) = A^0_{\text{ef},i} \cdot \left[1 + \lambda_i (p - p_{\text{ref}})\right] \cdot \left[1 + \alpha_i (T - T_{\text{ref}})\right] \tag{10}$$

where: $A^0_{\text{ef},i}$ – effective area under reference conditions (p_0, T_{ref}), λ_i – pressure distortion coefficient [10, 11], α_i – combined thermal coefficient.

Taking the above into account, the final measurement equation takes the form:

$$A^0_{\text{ef,DUT}} = A^0_{\text{ef,ST}} \cdot \eta_{\text{med}} \cdot R_v \cdot K_{\text{p}} \cdot K_{\text{T}} \cdot (1 + \Delta) \tag{11}$$

where: $A^0_{\text{ef,DUT}}$ – effective area of DUT at reference conditions $(p_{\text{ref}}, T_{\text{ref}})$ [m²], $A^0_{\text{ef},ST}$ – effective area of standard at reference conditions [m²], η_{med} – medium coefficient (1 for liquid medium, $\rho_{\text{ST}} / \rho_{\text{DUT}}$ for gaseous medium), R_v – flow rate change ratio: $\Delta v_{\text{ST}} / \Delta v_{\text{DUT}}$, K_{p} – pressure distortion factor, K_{T} – thermal coefficient factor, Δ – second-order correction factor – minor corrections arising from deviations from the ideal model.

The pressure distortion factor is defined as [16]:

$$K_{\text{p}} = \frac{1 + \lambda_{\text{ST}}(p_{\text{ST}} - p_{\text{ref}})}{1 + \lambda_{\text{DUT}}(p_{\text{DUT}} - p_{\text{ref}})} \tag{12}$$

where: λ_{ST} – standard pressure distortion coefficient (from calibration certificate) [Pa^{-1}], λ_{DUT} – DUT pressure distortion coefficient [Pa^{-1}], p_{ST} – standard pressure [Pa], p_{DUT} – DUT pressure [Pa], p_{ref} – reference pressure (usually the middle of the measurement range) [Pa].

Thermal coefficient factor is defined as:

$$K_{\text{T}} = \frac{1 + \alpha_{\text{ST}}(T_{\text{ST}} - T_{\text{ref}})}{1 + \alpha_{\text{DUT}}(T_{\text{DUT}} - T_{\text{ref}})} \tag{13}$$

where: α_{ST} – standard combined thermal coefficient [K^{-1}], α_{DUT} – DUT combined thermal coefficient [K^{-1}], T_{ST} – standard temperature [K], T_{DUT} – DUT temperature [K], T_{ref} – reference temperature [K].

Second-order correction factor is defined as:

$$\Delta = \delta_{\text{V}} + \delta_{\omega} + \delta_{\sigma} + \delta_{\text{al}} + \delta_{\text{inert}} + \delta_{\text{ad}} \tag{14}$$

where: δ_{V} – volume correction – arising from deviations from the ideal incompressibility of the medium, δ_{ω} – rotation correction – the change in leakage flow Q_{L} due to the differences of the piston's rotational speed between measurement intervals, δ_{σ} – surface tension correction (≡ 0 for gas), δ_{al} – alignment correction – cosine errors arising from the vertical alignment of the assemblies and the axes of the sensors, δ_{inert} – inertial correction – deviation from the floating equilibrium condition during transient states, δ_{ad} – adiabatic correction (gas only) – the effect of gas cooling during expansion through the valve.

Under the adopted assumptions, the oil was treated as an incompressible and temperature-invariant medium. However, in reality its properties are never ideal, and therefore these two parameters must be estimated for the purpose of the uncertainty budget. The compressibility of the oil may be assumed [14] at the level of $\kappa \approx 5 \cdot 10^{-10}\,\mathrm{Pa}^{-1}$, and its thermal expansion coefficient at $\beta_{\mathrm{ol}} \approx 7 \cdot 10^{-4}\,\mathrm{K}^{-1}$. When pressure or temperature changes transiently, additional flow contributions are generated within the volume V_i :

$$Q_{\mathrm{V},i} = \kappa \cdot V_i \cdot \frac{dp_i}{dt} - \beta_{\mathrm{ol}} \cdot V_i \cdot \frac{dT_i}{dt} \tag{15}$$

where: $Q_{\mathrm{V},i}$ – additional volumetric flow due to oil compressibility and thermal expansion [m³/s], κ – isothermal compressibility of the oil [Pa⁻¹], V_i – volume under the piston [m³], β_{ol} – volumetric thermal expansion coefficient of the oil [K⁻¹], dp_i / dt – rate of pressure change [Pa/s], dT_i / dt – rate of temperature change [K/s].

The correction to the measurement equation is given by:

$$\delta_{\mathrm{V}} = \frac{Q_{\mathrm{V,ST}} - Q_{\mathrm{V,DUT}}}{A_{\mathrm{ef,DUT}} \cdot \Delta v_{\mathrm{DUT}}} \tag{16}$$

where: $Q_{\mathrm{V,ST}}$ – additional volumetric flow in the standard chamber [m³/s], $Q_{\mathrm{V,DUT}}$ – additional volumetric flow in the DUT chamber [m³/s].

The leakage flow Q_{L} in the piston–cylinder clearance depends on the piston rotational speed. In instruments not equipped with a mechanical rotation-maintaining system, the rotational speed decreases, which implies that the parameter Q_{L} does not cancel identically:

$$\delta_{\omega} = \frac{\frac{\partial Q_{\mathrm{L}}}{\partial \omega} \cdot \Delta\omega}{A_{\mathrm{ef,DUT}} \cdot \Delta v_{\mathrm{DUT}}} \tag{17}$$

where: δ_{ω} – rotational correction due to decay of motion (typically ~2 ppm), $\partial Q_{\mathrm{L}} / \partial \omega$ – sensitivity of the leakage flow to rotational speed [m³ · s/rad], $\Delta\omega$ – change in rotational speed between measurement intervals [rad/s].

The surface tension of the oil introduces an additional contribution to the pressure beneath the piston, $\sigma C/A$. It can be assumed that the piston circumferences are different for the standard and the calibrated assembly. In that case:

$$\delta_{\sigma} = \frac{\sigma}{p_{\mathrm{ref}}} \cdot \left(\frac{C_{\mathrm{ST}}}{A_{\mathrm{ef,ST}}} - \frac{C_{\mathrm{DUT}}}{A_{\mathrm{ef,DUT}}} \right) \tag{18}$$

where: σ – oil surface tension (≈ 30 · 10⁻³ N/m) [N/m], C_{ST} – standard piston circumference [m], C_{DUT} – DUT piston circumference [m].

The contribution of this correction decreases inversely with p_{ref}, which makes it significant only for low-pressure measurement assemblies (range < 1 MPa). For gas $\sigma \equiv 0$.

The displacement sensor measures distance along the axis of the laser beam. If the sensor axis is inclined from the vertical by an angle θ, and the piston axis is inclined relative to the beam axis by an angle φ, then the true velocity along the cylinder axis is given by:

$$v = \frac{dz / dt}{\cos\theta \cdot \cos\varphi} \tag{19}$$

where: dz/dt – measured displacement rate (along sensor axis) [m/s], θ – angle of deviation of the laser beam axis from the vertical [rad], φ – angle of deviation of the piston axis from the vertical [rad].

For a precisely aligned setup (θ, φ < 1 mrad), the correction is negligibly small. However, for completeness, it should be included for the purposes of the uncertainty budget.

Immediately after opening the separating valve, a change in the fall velocity occurs. The resulting transient acceleration gives rise to an inertial force $M \cdot \frac{dv}{dt}$, which slightly disturbs the stable piston behaviour [17]. The correction associated with this phenomenon can be expressed as:

$$\delta_{\mathrm{inert}} = \frac{M_{\mathrm{DUT}} \cdot \frac{dv_{\mathrm{DUT}}}{dt} - M_{\mathrm{ST}} \cdot \frac{dv_{\mathrm{ST}}}{dt}}{A_{\mathrm{ef}} \cdot p} \tag{20}$$

where: δ_{inert} – inertial correction – deviation from quasi-steady-state conditions, $M_{\mathrm{ST/DUT}}$ – mass of the piston together with the weights of the given measurement assembly [kg], $dv_{\mathrm{ST/DUT}} / dt$ – piston acceleration in the transient state [m/s²], A_{ef} – effective area [m²], p – working pressure [Pa].

Appropriate selection of measurement data makes it possible to eliminate the need to account for the influence of this correction on the final results. However, an uncertainty contribution associated with the proper selection of the interval remains, although its magnitude is relatively small, typically below 1 ppm.

After opening the valve, the gas flowing between the chambers undergoes a locally quasi-adiabatic expansion, which temporarily reduces its temperature. The temperature field returns to equilibrium with a characteristic time constant τ_{term} (dependent on the thermal insulation of the chambers). If τ_{term} is comparable to τ_{meas}, a contribution arises

$$\delta_{\mathrm{ad}} \sim \frac{\gamma - 1}{\gamma} \cdot \frac{\tau_{\mathrm{term}}}{\tau_{\mathrm{meas}}} \cdot \frac{\Delta p}{p} \tag{21}$$

where: γ – adiabatic coefficient: $\gamma = c_p / c_v$ (for N_2 ≈ 1.4), τ_{term} – thermal relaxation time of the PCU chambers [s], τ_{meas} – measurement window [s], $\Delta p / p$ – relative pressure difference driving the flow through the valve.

The piston fall rate is determined indirectly by measuring the position $z(t)$ of a reference point on the stack of weights using a displacement sensor (laser, capacitive, or inductive [18, 19]). Piston displacement was measured using two Micro-Epsilon ILD1420-25 triangulation laser sensors with a measuring range of 0–25 mm, mounted individually for the standard and the DUT. The sensors were connected to a C-Box/2A controller via RS-422 interfaces. The C-Box/2A provided a common internal time base and synchronized both measurement channels in a master–slave configuration, thereby minimizing the relative time offset between the recorded signals [20]. The velocity is obtained by fitting a straight line to the recorded trajectory using the least-squares method:

$$z(t) = z_0 + v \cdot t \tag{22}$$

where: $z(t)$ – current position of the reference point on the stack of weights [m], z_0 – starting position [m], v – piston velocity – the slope of the line fitted [m/s].

An important advantage of the proposed method is the possibility of independently adjusting the initial position for each measurement point. As a result, there is no need to maintain an absolute starting distance. This implies that the influence of temperature on the height of the weight stack becomes negligible (with contribution to the uncertainty of the velocity ratio R_v below 1 ppm). However, correct synchronization of the recorded sensor signals is critical. This can be achieved in two ways: via hardware synchronization or by means of mathematical processing. The data recorded by the sensors can be divided into three stages: the free-fall phase of the assemblies (prior to valve opening), the transient phase (immediately after valve opening, dominated by inertial effects), and the evaluation phase, in which the fall/rise velocity decays continuously as the pistons travel toward their end-stops, and from which only the early, approximately linear segment (after the inertial guard interval) is used to determine the velocity difference.

3.2. Measurement procedure

Phase 0 – selection of measurement points. At least five measurement points should be selected, evenly distributed across the entire measurement range of the piston–cylinder assembly. The measurement system is then connected and the displacement sensors are activated. Environmental conditions are verified (ambient temperature: 20 ±1 °C, relative humidity: 50 ±30 %).

Phase 1 – preparation of the measurement system for data acquisition, i.e. loading the pistons with the appropriate weights, setting the assemblies to their operating positions, initiating rotation, verifying the correctness of the nominal fall velocity, and verifying the thermal stability of the setup. The appropriate piston positions are established (maximum available travel range).

Phase 2 – recording of the natural fall velocity. This period must not be too short, in order to ensure that the measurement results are not distorted by possible transient disturbances. In practice, this means an acquisition lasting at least 10 seconds at the sampling rate of 1 kHz which makes it sufficient for minimizing the error of calculation the fitted natural fall rate and making its contribution insignificant in the uncertainty budget of the R_v.

Phase 3 – opening of the valve and recording of piston displacement for at least a sufficient duration. The acquisition time must not be too short, as part of the data (immediately after valve opening) cannot be included in the calculations due to inertial effects. Typically, an interval of approximately 1–3 seconds is excluded from the evaluation. Again acquisition lasting at least 10 s at the sampling rate of 1 kHz should take place.

Phase 4 – processing of the collected data and analysis of the obtained results.

Data acquisition using sensors should be performed in such a way that the number of recorded samples enables statistical averaging. The minimum number of samples is 1000; however, an optimal dataset should contain more than 10,000 samples.

3.3. Uncertainty budget

In general terms, the analysis of uncertainty components in the calibration of pressure balances (dead-weight piston gauges) is a highly extensive topic and may involve from a dozen to several dozen contributing factors, depending on the level of detail and accuracy required. Figure 2 presents a compilation of influencing factors whose presence should be considered as affecting the calibration process using the Extended Cross-Float method. Not all of these factors are sufficiently significant to be included in quantitative calculations. However, the majority represent a level of importance that substantially affects the final uncertainty. Their analysis is presented in the subsequent sections of the text.

Due to the multiplicative nature of the measurement equation, a relative formulation was adopted. The contribution of each component is expressed as:

$$\frac{u_j(A^0_{\mathrm{ef,DUT}})}{A^0_{\mathrm{ef,DUT}}} = \left|c_j\right| \cdot \frac{u(x_j)}{x_j} \tag{23}$$

where c_j is the sensitivity coefficient (for factors in a product $c = \pm 1$) [4]. The combined uncertainty is expressed as:

$$\frac{u_c(A^0_{\mathrm{ef,DUT}})^2}{A^0_{\mathrm{ef,DUT}}} = \sum \left[c_j \cdot \frac{u(x_j)}{x_j} \right]^2 \tag{24}$$

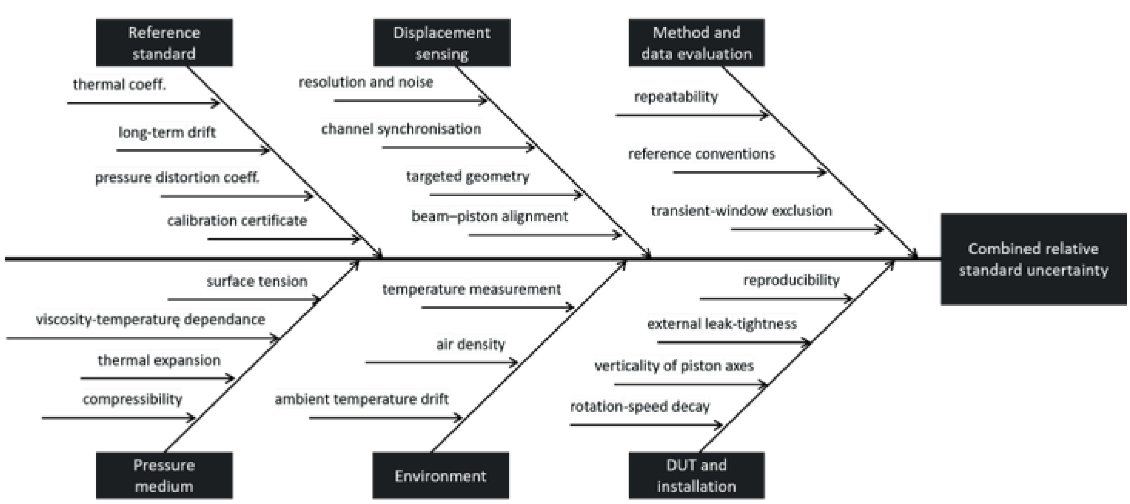

Fig. 2. Uncertainty components for Extended Cross-Float calibration method

Rys. 2. Składowe niepewności w rozszerzonej metodzie wzorcowania cross-float

Table 1. Uncertainty budget for Extended Cross-Float calibration method
Tabela 1. Budżet niepewności rozszerzonej metody wzorcowania cross-float

Quantity X_i	Estimate x_i	Standard uncertainty $u(x_i)$	Probability distribution	Sensitivity coefficient c_i	Uncertainty contribution $u_i(y)$ [ppm]
$A^0_{\mathrm{ef},ST}$	From certificate	$U_{\mathrm{cert}}/2$	Normal	+1	≈ 25
A^0_{ef} reproducibility (between-point and between-series, Type A, dominant):				**+1**	**≈ 625**
between-point and between-series scatter of the six A_{ef} values	A^0_{ef}	s/√n (sample SD of the six A_{ef} values)	Normal (t-dist., $\nu = n-1$)	+1	625
R_{v} (velocity ratio – within-run):				**+1**	**≈ 33**
$R_{\mathrm{v,rep}}$ – repeatability (rolling TLS, settled window)	$R_{\mathrm{v,settled}}$	$s(R_{\mathrm{v}}(t))/\sqrt{N_{\mathrm{eff}}}$	Normal (t-dist.)	+1	30
$R_{\mathrm{v,res}}$ – sensor resolution	0	$\sqrt{2} \cdot u(z)/(v \cdot T) \cdot \sqrt{(N/12)}$	Rectangular	+1	5
$R_{\mathrm{v,lin}}$ – sensor linearity (differential, slope-based)	0	±0.05 % · range · √2/√3 (differential)	Rectangular	+1	12
K_{p} (pressure distortion):				**+1**	**≈ 25**
$u(\lambda)$ – distortion coeff. (from certificate)	λ_{ST}, λ_{DUT}	$U(\lambda)/k = 0.5\times10^{-7}\ \mathrm{Pa}^{-1}$	Normal	$\lvert p-p_{\mathrm{ref}}\rvert$	24
$u(p)$ – pressure	p_{ST}, p_{DUT}	5 ppm of p	Normal	$\lambda \cdot p$	< 1
K_{T} (thermal coefficient):				**+1**	**≈ 17**
$u(T)$ – temperature (20 ±1 °C control)	20 °C	0.58 K (rect. ±1 °C)	Rectangular	$\alpha \cdot \lvert T - T_{\mathrm{ref}}\rvert$	≈ 12 (each)
$u(\alpha)$ – thermal coefficient	≈ $20\times10^{-6}\ \mathrm{K}^{-1}$	$1\times10^{-6}\ \mathrm{K}^{-1}$	Rectangular	ΔT	1
$u(\Delta T_{\mathrm{ST-DUT}})$ – temperature difference	0 K	0.12 K (rect. ±0.2 K)	Rectangular	$\alpha \cdot \Delta T$	4
η_{med} (medium coeff.)				**+1**	**≈ 10**
residual after hydrostatic height correction	1	residual of $\rho \cdot g \cdot \Delta h/p$ correction	Rectangular	+1	10
Δ (second-order corrections):				**+1**	**≈ 6**
δ_{V} – oil compressibility	0	$\kappa \cdot V \cdot (dp/dt)/A_{\mathrm{ef}} \cdot \Delta v \cdot \sqrt{3})$	Rectangular	+1	5
δ_{ω} – rotation speed decay	0	$\partial Q_{\mathrm{L}}/\partial\omega \cdot \Delta\omega/(A_{\mathrm{ef}} \cdot \Delta v \cdot \sqrt{3})$	Rectangular	+1	2
δ_{σ} – surface tension (oil)	0	$\sigma \cdot \Delta C/(p \cdot A_{\mathrm{ef}} \cdot \sqrt{3})$	Rectangular	+1	3
δ_{al} – sensor/piston alignment (cosine error)	0	$(\theta^2 + \varphi^2)/2 \cdot (1/\sqrt{3})$	Rectangular	+1	1
δ_{inert} – inertia (guard 1–3 s post-valve)	0	$M \cdot \mathrm{d}v/dt/(A_{\mathrm{ef}} \cdot p \cdot \sqrt{3})$	Rectangular	+1	< 1
$A^0_{\mathrm{ef,DUT}}$ (standard)	computed	u_c			≈ 627
$A^0_{\mathrm{ef,DUT}}$ (combined, $k = 2$)	computed				**≈ 1250**

$$U(A^0_{\mathrm{ef,DUT}}) = 1.25 \cdot 10^{-3} \cdot A^0_{\mathrm{ef,DUT}}$$

Because the measurement equation (11) is a product of factors, a relative uncertainty formulation is adopted. The combined relative standard uncertainty of $A^0_{\mathrm{ef,DUT}}$ is:

$$\left[u(A^0_{\mathrm{ef,DUT}})\right]^2 = u(A^0_{\mathrm{ef,ST}})^2 + u(R_v)^2 + u(K_\mathrm{p})^2 + u(K_\mathrm{T})^2 + u(\eta_\mathrm{med})^2 + u(\Delta)^2 \tag{25}$$

where $u(x_i) = u(x_i)/|x_i|$ is the relative standard uncertainty of input quantity x_i. All sensitivity coefficients c_i equal ±1 for factors in a product. The terms are assumed to be uncorrelated. The expanded relative uncertainty is:

$$U(A^0_{\mathrm{ef,DUT}}) = k \cdot u_c(A^0_{\mathrm{ef,DUT}})$$

with $k = 2$ (coverage probability ≈ 95 %) (26)

4. Results

The measurements were carried out on a measurement setup equipped with two deadweight piston pressure gauge assemblies with a measurement range of 1–60 bar, which were manufactured for the purposes of this project. Three measurement series were performed at six measurement points corresponding to the following load masses: 5 kg, 10 kg, 15 kg, 20 kg, 25 kg and 30 kg, which equals to 10 bar, 20 bar, 30 bar, 40 bar, 50 bar and 60 bar. An example of measurements gathered during the calibration is presented in Figure 3.

For each measurement point a "pre-valve" and "post-valve" area has been selected. First is used for the detrend function after which the second is used to finally calculate effective area of the piston-cylinder assembly. The post-valve window is restricted to the initial quasi-linear segment immediately following the inertial guard interval, where the chamber pressures, and therefore the leakage flow Q_L, remain at their closed-valve values. The later saturating part of the record, where the pistons approach their end-stops and Q_L drifts, is excluded, because in that region the cancellation of Q_L between equations (3) and (4) no longer holds.

After opening the shut-off valve, the piston motions remain hydraulically coupled through the common pressure-transmitting medium. Since no additional outflow path is created apart from the existing piston–cylinder clearances, the volume displaced by one piston must be balanced by the motion of the other piston and the corresponding clearance flows. Consequently, the piston displacements are not independent but form a uniquely determined coupled response to the pressure imbalance. Over the selected evaluation interval, this response may be treated as approximately linear, although the piston velocities gradually change as the pressure difference decreases. Other influence quantities, such as medium properties or piston–cylinder geometry, may affect the magnitude and time evolution of the velocities, but they act symmetrically on both sides of the system and do not alter this mutual dependence.

Because the measured pressure dependence is well below the observed scatter, the pressure distortion coefficient cannot be resolved, and $A^0_{\mathrm{ef,DUT}}$ is reported as the mean of the points over the range rather than as a regression intercept. Six measurement points resulted in values presented in Figure 4 and Table 2:

The results in Table 2 lead to a following observations. The six values of $A_{\mathrm{ef,DUT}}$ show no clear dependence on pressure, and none of them deviates from the mean by more than twice the between-point standard deviation (approx. 0.0006 cm², i.e. approx. 0.12 %), so the scatter is statistically consistent and contains no outliers. It is this scatter, and not the systematic (Type B) effects, which together amount to only approx. 0.01 % at $k = 2$, that limits the combined uncertainty. The per-point uncertainties decrease with pressure, from approx. 0.05 % at 10 bar to below 0.01 % at 60 bar, because at low loads the fall rates changes are small and their slopes are harder to determine precisely. An independent check of accuracy is provided by a classical cross-float calibration of the same assembly, which gave $A^0_{\mathrm{ef,DUT}} = 0.473661\,\mathrm{cm}^2$ with an expanded uncertainty of 0.000038 cm² ($k = 2$). The result of the Extended Cross-Float method differs from this value by only 0.000122 cm² (approx. 0.026 %), i.e. about one quarter of the combined expanded uncertainty of the two results (normalized error $E_n \approx 0.25$), and

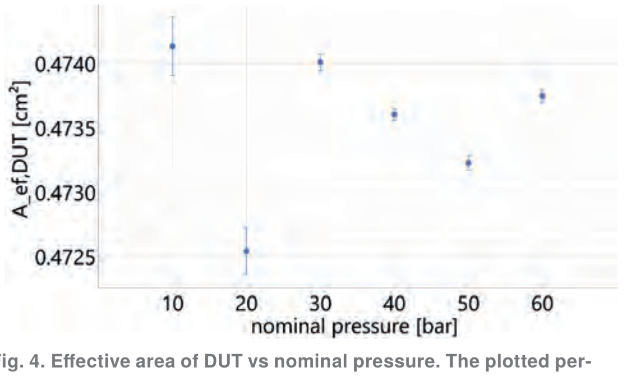

Fig. 4. Effective area of DUT vs nominal pressure. The plotted per-point bars represent the within-run uncertainty only (velocity-ratio repeatability and Type B terms). The point-to-point scatter exceeds these bars, which reflects the dominant between-point reproducibility entered in Table 1 and carried into $U(A^0_{\mathrm{ef,\,DUT}})$ in Table 2

Rys. 4. Przekrój czynny przyrządu wzorcowanego w funkcji ciśnienia nominalnego. Naniesione dla poszczególnych punktów słupki niepewności reprezentują wyłącznie niepewność w obrębie pojedynczej serii (powtarzalność stosunku prędkości oraz składowe typu B). Rozrzut między punktami przekracza te słupki, co odzwierciedla dominującą składową odtwarzalności między punktami pomiarowymi, ujętą w tab. 1 i uwzględnioną w $U(A^0_{\mathrm{ef,\,DUT}})$ w tab. 2.

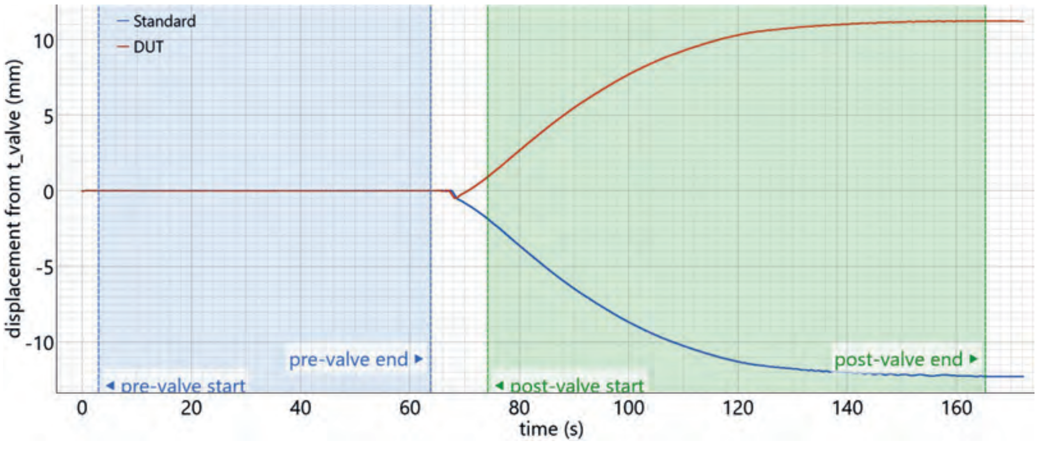

Fig. 3. Standard (blue line) and DUT (red line) displacement measurement

Rys. 3. Pomiar przemieszczenia wzorca (linia niebieska) i przyrządu wzorcowanego (linia czerwona)

Table 2. Final results of extended cross-float calibration
Tabela 2. Końcowe wyniki wzorcowania rozszerzoną metodą cross-float

Nominal pressure [bar]	$A_{\mathrm{ef,DUT}}$ [cm²]	$U(A_{\mathrm{ef,DUT}})$[cm²]
10	0.474129	0.000229
20	0.472537	0.000181
30	0.474005	0.000066
40	0.473599	0.000046
50	0.473222	0.000057
60	0.473742	0.000045
$A^0_{\mathrm{ef,DUT}}$ [cm²]	**0.473539**	**0.000489**

the reference value lies well within the uncertainty interval of the Extended Cross-Float result. Both methods are therefore metrologically consistent: the dynamic approach introduces no significant systematic error at its present uncertainty level, and its limitation is precision rather than trueness.

5. Conclusion

The results confirm that the Extended Cross-Float method works and that it delivers a clear practical advantage over the classical approach. By replacing the laborious search for a hydrostatic equilibrium point with a direct measurement of piston velocity, it removes the single most time-consuming stage of conventional calibration. It does not compete with the classical Cross-Float method but complements it naturally: used as a form of preselection, it can markedly accelerate the location of the equilibrium point, and, after modest refinement, it can also serve as a convenient tool to verify the readiness of a pressure measurement system for calibration. Because it reuses the standard and device-under-test arrangement already present in calibration laboratories, it is inexpensive to adopt and easy to put into routine practice.

The clearest direction for further development is reproducibility. The treatment of the calibration in a dynamic regime is demanding, and the present dispersion of results shows that there is meaningful room to improve. A likely contributor is that the post-valve velocity is not constant but decays as the pistons travel toward their end-stops, so a single fitted velocity difference depends on the chosen analysis window, which biases the velocity ratio between the two assemblies. Promising avenues therefore include refining the analytical tools, optimizing the design of the shut-off valve, and tightening control of environmental conditions, since the measurements are acquired over a relatively short interval in which any transient disturbance can have a disproportionate effect. These are well-defined, tractable steps, which makes the outlook for the method genuinely encouraging.

A distinctive feature of the Extended Cross-Float method, and one that sets it apart from the classical Cross-Float method, is the central role of the analytical methods and signal processing it employs. This is primarily a strength: well-chosen filtering and computational parameters give the method considerable flexibility and allow appropriate corrections and interpretations to be applied to real measurement data. It does mean that this stage deserves careful attention, since the quality of the processing directly shapes the quality of the final results, which is precisely why the analytical side offers such a promising route for further gains in accuracy.

In summary, the presented calibration method shows strong implementation potential and clear practical appeal, both as an additional approach for determining the effective cross-sectional area of pressure balance measuring systems (either as a standalone method or as complementary measurements) and in terms of its excellent prospects for further development. Its speed, simplicity, and low instrumentation cost make it a particularly attractive option for calibration laboratories seeking to streamline and de-risk the pressure-balance calibration process.

References

1. Stock M., Davis R., de Mirandés E., Milton M.J.T., *The revision of the SI – the result of three decades of progress in metrology*, "Metrologia", Vol. 56, No. 2, 2019, DOI: 10.1088/1681-7575/ab0013.
2. Olson D.A., Driver R.G., Bowers W.J., *A gas pressure scale based on primary standard piston gauges*, "Journal of Research of the National Institute of Standards and Technology", Vol. 115, No. 6, 2010, 393–412, DOI: 10.6028/jres.115.027.
3. Sabuga W., Rabault T., Wüthrich C., Pražák D., Chytil M., Brouwer L., Ahmed A.D., *High pressure metrology for industrial applications*, "Metrologia", Vol. 54, No. 6, 2017, DOI: 10.1088/1681-7575/aa895a.
4. Jousten K., Hendricks J., Barker D., Douglas K., Eckel S., Egan P., Fedchak J., Flügge J., Gaiser C., Olson D., Ricker J., Rubin T., Sabuga W., Scherschligt J., Schödel R., Sterr U., Stone J., Strouse G., *Perspectives for a new realization of the pascal by optical methods*, "Metrologia", Vol. 54, No. 6, 2017, DOI: 10.1088/1681-7575/aa8a4d.
5. Gaiser C., Fellmuth B., Sabuga W., *Primary gas-pressure standard from electrical measurements and thermophysical ab initio calculations*, "Nature Physics", Vol. 16, 2020, 177–180, DOI: 10.1038/s41567-019-0722-2.
6. Sharipov F., Yang Y., Ricker J.E., Hendricks J.H., *Primary pressure standard based on piston-cylinder assemblies: calculation of effective cross sectional area based on rarefied gas dynamics*, "Metrologia", Vol. 53, No. 5, 2016, DOI: 10.1088/0026-1394/53/5/1177.
7. Sabuga W., Priruenrom T., Molinar Min Beciet G., Giovinco G., Rabault T., Wongthep P., Pražák D., *FEA calculation of pressure distortion coefficients of gas-operated pressure balances – EURAMET project 1039*, "Measurement", Vol. 45, No. 10, 2012, 2464–2468, DOI: 10.1016/j.measurement.2011.10.035.
8. Thakur V.N., Sharipov F., Yang Y., Kumar S., Ram J., Omprakash H., Kumar H., Sharma R., Yadav S., Ashok Kumar, *Evaluation of effective area of air piston gauge with limitations in piston–cylinder dimension measurements*, "Metrologia", Vol. 58, No. 3, 2021, DOI: 10.1088/1681-7575/abe222.
9. Könemann J., Sabuga W., Pražák D., Rabault T., Wüthrich C., *Final report on supplementary comparison EURAMET.M.P-S14 of hydraulic gauge pressure standards from 50 MPa to 1000 MPa*, "Metrologia", Vol. 55, No. 1A, 2018, DOI: 10.1088/0026-1394/55/1A/07008.
10. Forssén C., Silander I., Zakrisson J., Amer E., Szabo D., Bock T., Kussike A., Rubin T., Mari D., Pasqualin S., Silvestri Z., Bentouati D., Axner O., Zelan M., *Demonstration of a transportable Fabry–Pérot refractometer by a ring-type comparison of dead-weight pressure balances at four European national metrology institutes*, "Sensors", Vol. 24, No. 1, 2023, DOI: 10.3390/s24010007.

11. Bermanec L.G., Zvizdic D., Simunovic V., Development of a method for the determination of the pressure balance piston fall rate, "Acta IMEKO", Vol. 3, No. 2, 2014, DOI: 10.21014/acta_imeko.v3i2.105.
12. Sharma R.K., Rab S., Kumar L., Zafer A., Yadav S., *Design and development of an indigenous cross-floating pressure calibration system up to 140 MPa*, "MAPAN – Journal of Metrology Society of India", Vol. 36, No. 2, 2021, 295–303, DOI: 10.1007/s12647-021-00450-4.
13. Rab S., Yadav S., Sharma R.K., Kumar L., Gupta V.K., Zafer A., Haleem A., *Development of hydraulic cross floating valve*, "Review of Scientific Instruments", Vol. 90, No. 8, 2019, DOI: 10.1063/1.5089953.
14. Ehlers S., Könemann J., Ott O., Wolf H., Šetina J., Furtado A., Sabuga W., *Selection and characterization of liquids for a low pressure interferometric liquid column manometer*, "Measurement", Vol. 132, 2019, 191–198, DOI: 10.1016/j.measurement.2018.09.017.
15. Hashad A.S., Ehlers S., Jusko O., Sabuga W., *Characterization of a force-balanced piston gauge as a primary pressure standard*, "Measurement", Vol. 131, 2019, 723–729, DOI: 10.1016/j.measurement.2018.09.016.
16. Singh J., Kumaraswamidhas L.A., Kaushik K., Bura N., Sharma N.D., *Uncertainty analysis of distortion coefficient of piston gauge using Monte Carlo method*, "MAPAN – Journal of Metrology Society of India", Vol. 34, No. 3, 2019, 379–385, DOI: 10.1007/S12647-019-00305-z.
17. Zafer A., Yadav S., Sanjid A., Kumar L., Sharma R.K., *Volume ratio and pressure drop on hydraulic dynamic pressure calibration system*, "Journal of Mechanical Science and Technology", Vol. 31, 2017, 3769–3775, DOI: 10.1007/s12206-017-0720-1.
18. Egan P.F., Stone J.A., Ricker J.E., Hendricks J.H., *Comparison measurements of low-pressure between a laser refractometer and ultrasonic manometer*, "Review of Scientific Instruments", Vol. 87, No. 5, 2016, DOI: 10.1063/1.4949504.
19. Cui C., Li X., *Precision nanometrology: laser interferometer, grating interferometer and time grating sensor*, "Sensors", Vol. 25, No. 21, 2025, DOI: 10.3390/s25216791.
20. Brzozowski A., Szewczyk R., Gazda P., Nowicki M., *Functional parameters of sensors for the Extended Cross-Float method*, "Metrology and Measurement Systems", Vol. 31, No. 4, 2024, 863–873, DOI: 10.24425/mms.2024.152056.

Wzorcowanie rozszerzoną metodą wzajemnego równoważenia

Streszczenie: W artykule przedstawiono rozszerzoną metodę wzajemnego równoważenia (ang. Extended Cross-Float) – nową propozycję wzorcowania zespołów tłok-cylinder ciśnieniomierzy obciążnikowo-tłokowych, stanowiącą alternatywę dla klasycznej metody równoważenia wzajemnego. W odróżnieniu od podejścia konwencjonalnego, w którym niezbędne jest doświadczalne wyznaczenie punktu równowagi hydrostatycznej w drodze iteracyjnego dobierania mas, w metodzie proponowanej przekrój czynny zespołu wzorcowanego wyznaczany jest w ujęciu dynamicznym – na podstawie zmiany prędkości opadania tłoka, rejestrowanej przed otwarciem i po otwarciu zaworu rozdzielającego. Sformułowano pełny model pomiaru wraz z odpowiadającym mu budżetem niepewności, a zasadę działania metody zweryfikowano eksperymentalnie na stanowisku badawczym w zakresie ciśnień typowym dla zastosowań laboratoryjnych. Uzyskane rezultaty potwierdzają poprawność przyjętych założeń i wskazują na potencjał metody zarówno jako narzędzia selekcji wstępnej, skracającego procedurę wzorcowania, jak i niezależnego sposobu weryfikacji uzyskanych wyników. Ograniczone wymagania aparaturowe sprawiają, że metoda może być wdrożona w istniejących stanowiskach laboratoriów wzorcujących.

Słowa kluczowe: wzorcowanie, ciśnieniomierz obciążnikowo-tłokowy, metrologia ciśnienia, wzorcowanie zespołów tłok-cylinder, rozszerzona metoda wzajemnego równoważenia, wyznaczanie przekroju czynnego

Adam Brzozowski, MSc Eng.

adam.brzozowski@gum.gov.pl
ORCID: 0000-0001-9488-9696

Deputy Director of the Department of Mechanics and Acoustics at the Central Office of Measures, PhD student in an implementation doctorate program at the Warsaw University of Technology. Specializes in metrology, calibration and measurement methods, uncertainty budget, particularly in the field of pressure and dynamic pressure.

Piotr Gazda, PhD Eng.

piotr.gazda@pw.edu.pl
ORCID: 0000-0002-6017-6134

His research focuses on the development of measurement methods and the design of innovative test stands, with particular emphasis on magnetoelectric phenomena. He is also engaged in the application of artificial intelligence to measurement systems. He defended his doctoral dissertation with distinction in 2020 and currently holds the position of assistant professor at the Institute of Metrology and Biomedical Engineering, Warsaw University of Technology.

Michał Nowicki, PhD Eng.

michal.nowicki@pw.edu.pl
ORCID: 0000-0003-2513-952X

Assistant professor at the Department of Sensors and Measurement Systems, Institute of Metrology and Biomedical Engineering, Warsaw University of Technology. He specializes in the design and construction of experimental measurement systems, in particular magnetic and magnetomechanical ones, and the development of new sensor structures. Privately, he is interested in technical archeology and exotic technologies.